Supporting Information

Enhancing Quantum Yield in Strained MoS_2 Bilayers by Morphology-controlled Plasmonic Nanostructures towards Superior Photodetectors

*Pavithra Sriram [a], Yu-Po Wen [a], Arumugam Manikandan [a], Kun-Chieh Hsu [b], Shin-Yi Tang [a], Bo-Wei Hsu [a], Yu-Ze Chen [a], Hao-Wu Lin [a], Horng-Tay Jeng [b], Yu-Lun Chueh [a], Ta-Jen Yen [a]**

[a] Department of Materials Science and Engineering, National Tsing Hua University, Hsinchu, 30013, Taiwan, R.O.C.

[b] Department of Physics, National Tsing Hua University, Hsinchu, 30013, Taiwan, R.O.C.

***Corresponding author**

Prof. Ta-Jen Yen, E-mail: tjyen@mx.nthu.edu.tw

a) CVR-grown bilayer MoS_2 and chemically synthesized Au nanostructures:

Figure S1a shows the shows the Raman spectrum of bilayer MoS_2 with characteristic peaks of the in-plane Raman mode (E^1_{2g}) and the out-of-plane Raman mode (A_{1g}) at the frequencies of 384.2 cm^{-1} and 406.4 cm^{-1}, respectively with 22.2 cm^{-1} distance between two modes[1] confirming the growth of bilayer MoS_2. Figure S1b presents the UV-visible absorption spectrum of Au nanoparticles with various morphologies overlapping with the incident excitation wavelength. We tailored the size of the nanoparticles to employ the spectral overlap between localized surface plasmon resonances (LSPRs) of Au nanoparticles and the incident excitation wavelength (520 nm).

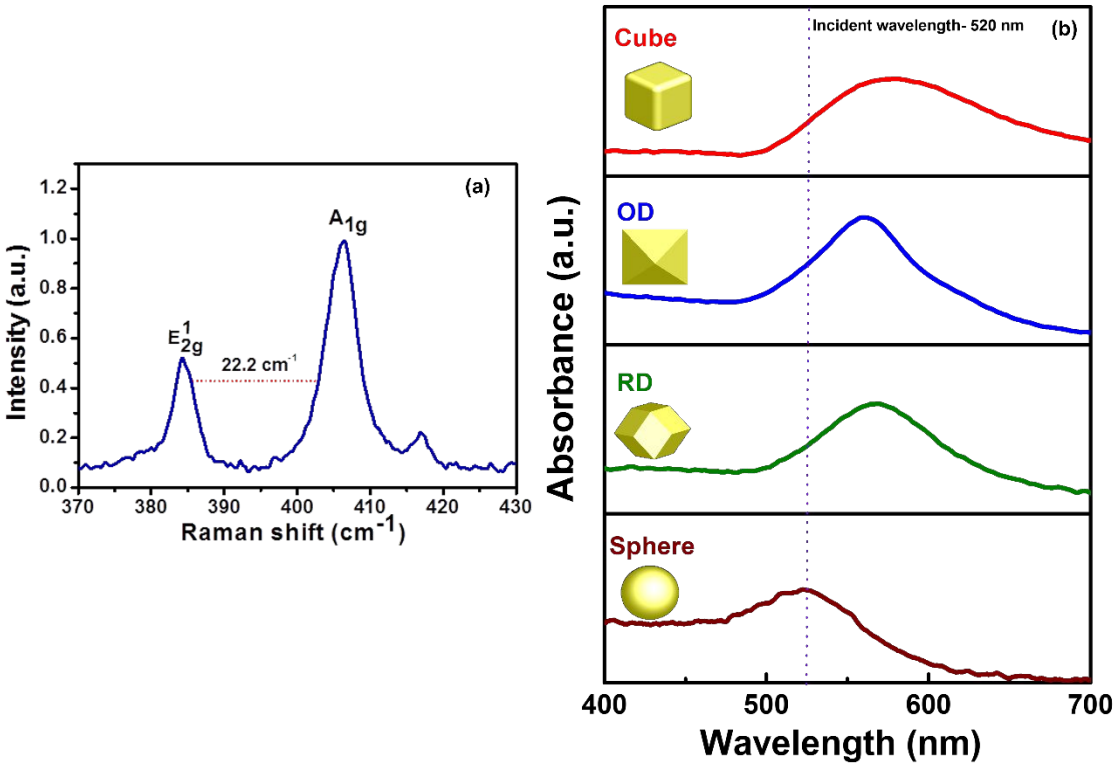

Figure S1. a) Raman spectrum of bilayer MoS_2 on a sapphire substrate; b) UV-vis absorption spectra of various nanostructures (the dashed vertical line corresponds to the laser excitation wavelength).

b) Size distribution histograms of Au nanostructures:

The size distribution maps of Au nanoparticles of various shapes are shown in Figure S2. The average size of nanocubes ~ 83 nm; octahedra ~ 74 nm; Rhombic dodecahedra ~ 64 nm; Nanorods ~ length - 65 nm; width - 23 nm. The histogram plot demonstrates the uniform sizes of chemically synthesized Au nanoparticles.

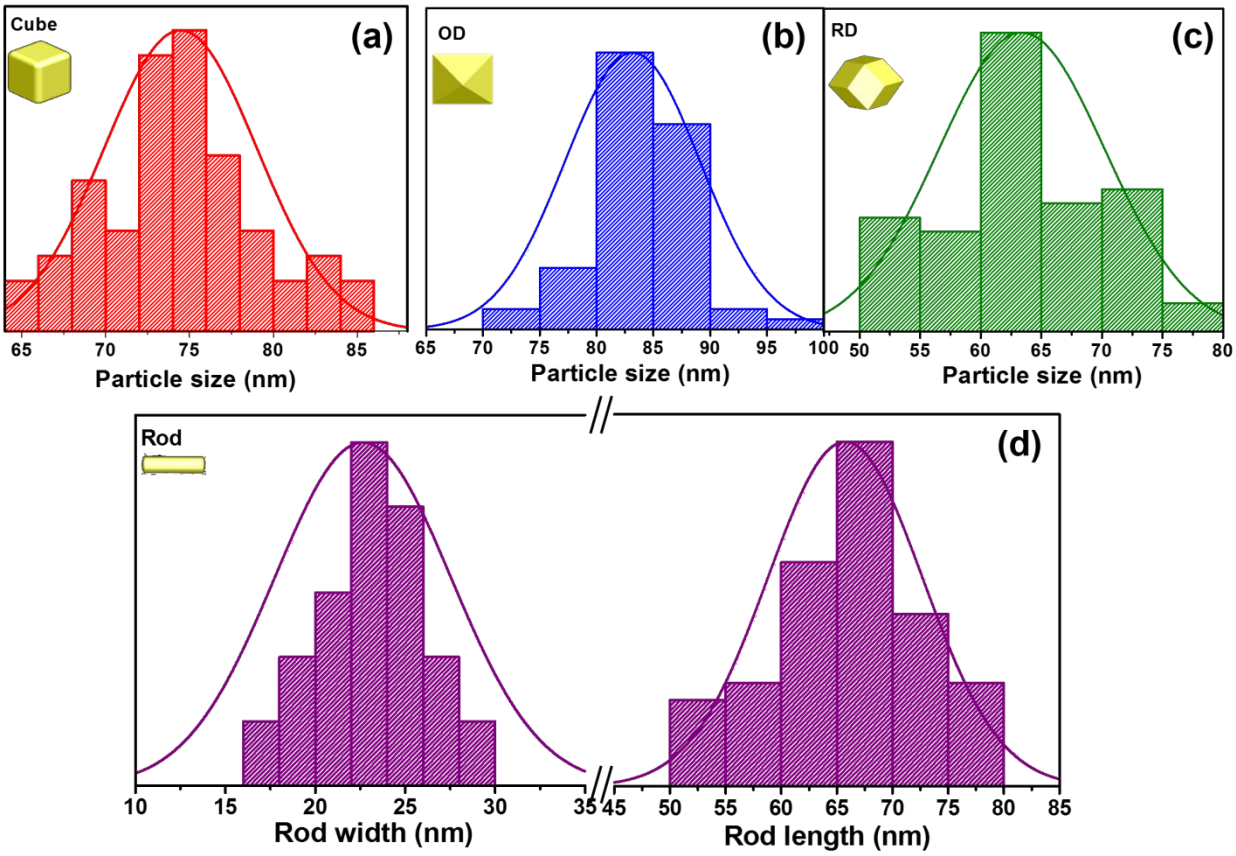

Figure S2. Size distribution histograms of Au nanostructures. (a) Nanocubes; (b) Octahedra; (c) Rhombic dodecahedra; (d) Nanorods.

c) XY-field distributions of bilayer MoS_2 interfaces with various Au nanostructures:

Au nanocube being symmetric structures, the longitudinal and transverse mode of Au nanocube substantially degenerate, resulting in a ring-like plasmonic mode. While the nanorod with high-aspect-ratio, breaks this degeneracy and creates longitudinal & transverse mode. For complex nanostrcutures such as OD and RD electric field are concentrated at the vertices. Au sphere has small interface area with MoS_2 resulting in limited e-field confined region.

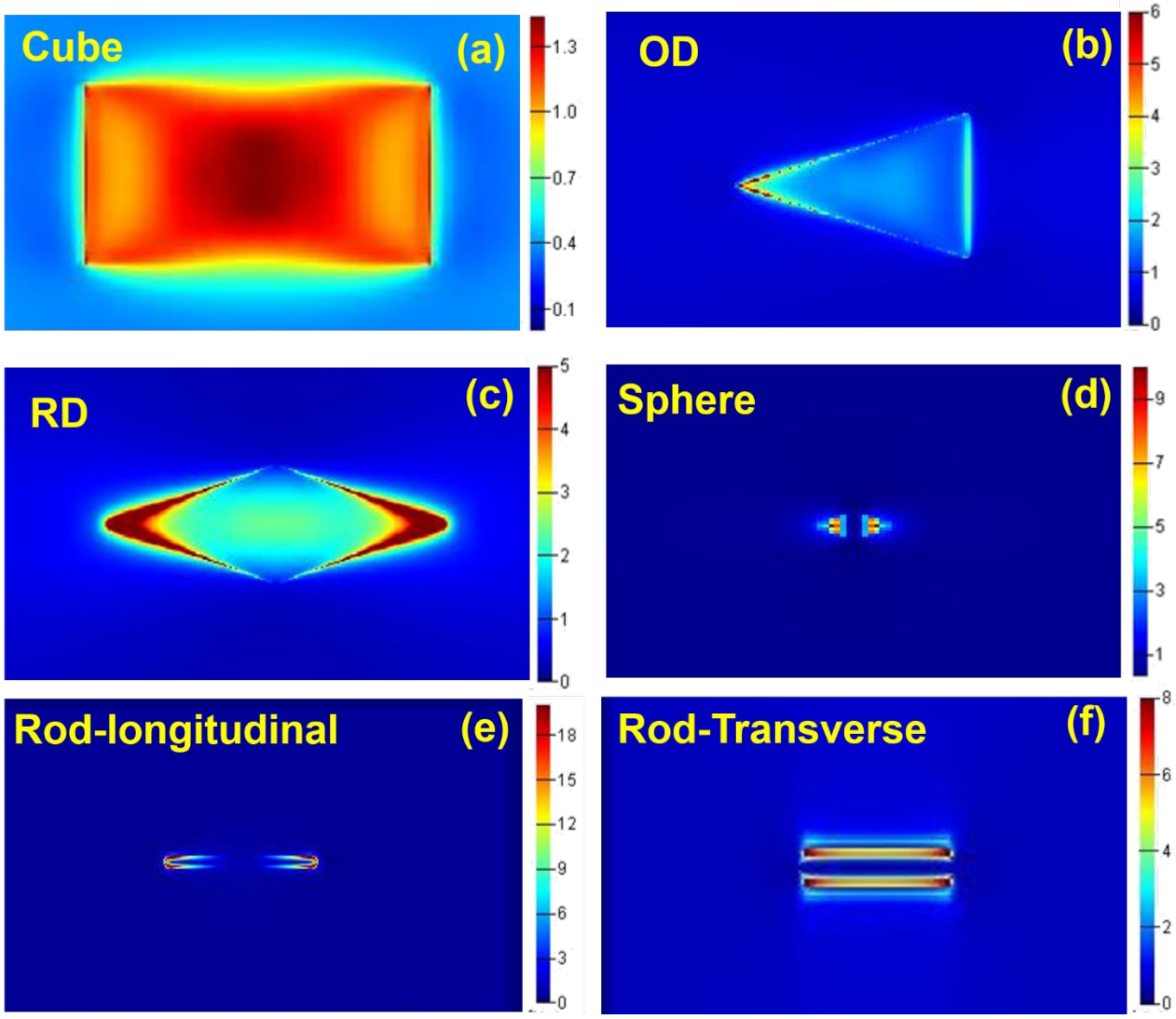

Figure S3. FDTD-simulated XY-field distributions of bilayer MoS_2 interfaces with various Au nanostructures.

d) Prolonged time-resolved photoresponse performance of the hybrid device:

we performed time-resolved evolution of our bilayer MoS_2, which was integrated with the plasmonic structure with laser on/off modes for a prolonged time for V_{ds} = 10 V and P = 318.471 mW/cm^2, as shown in Figure S4. We observe a gentle increase in the photocurrent under laser illumination and a sharp drop due to pacific relaxation when the laser is switched off. The rising time of our device is estimated to be 0.26 s and the decay time is 0.45 s. The rising and decay times of our device show significant improvement compared to the Pt-strip-enabled MoS_2 bilayer[2].

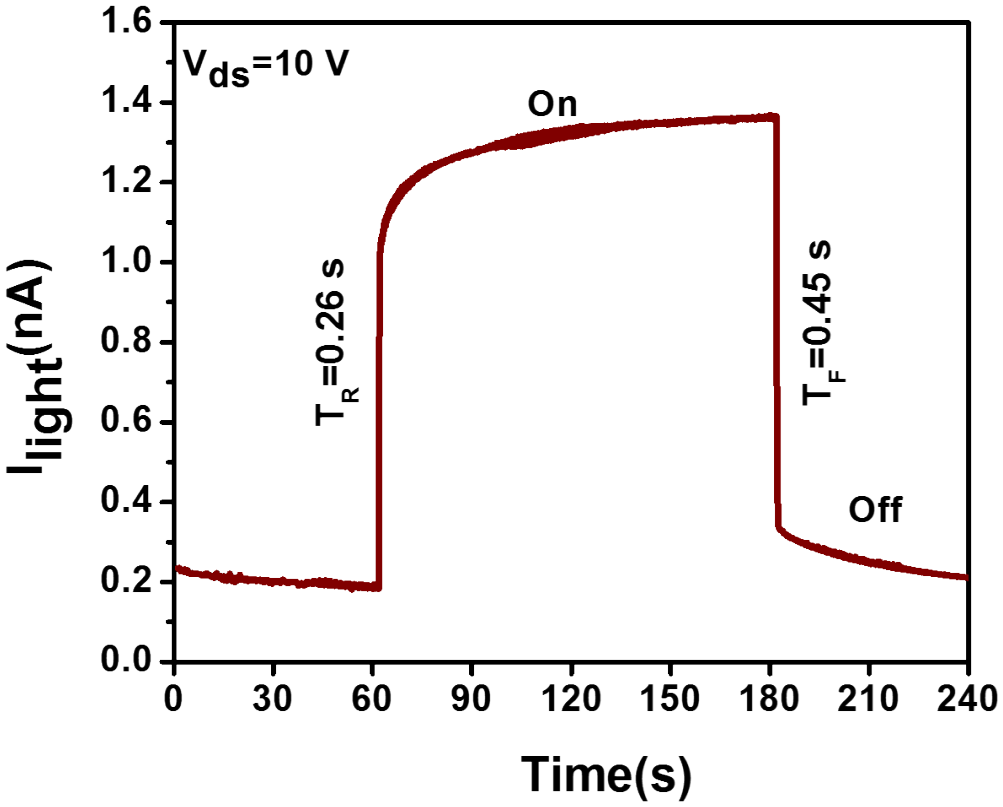

Figure S4: Prolonged time-resolved photoresponse performance of the hybrid MoS2-Au nanocube device at V_{ds} = 10 V; laser power density = 318.471 mW/cm^2.

e) The photoresponsivity measurement of hybrid MoS_2 bilayer with other Au-OD & RD:

The photoresponsivity measurement of hybrid MoS_2 bilayer with other Au nanostructures such as Au-OD and RD has been carried out, and the results are displayed in Figures S5. The plot of photocurrent versus time of bilayer MoS_2 that is decorated with Au OD & RD at various bias voltages (V_{ds} = 1,3,5,7,10 V) demonstrates the reproducibility and consistent behavior of our hybrid as-grown bilayer MoS_2 that is decorated with Au nanostructures.

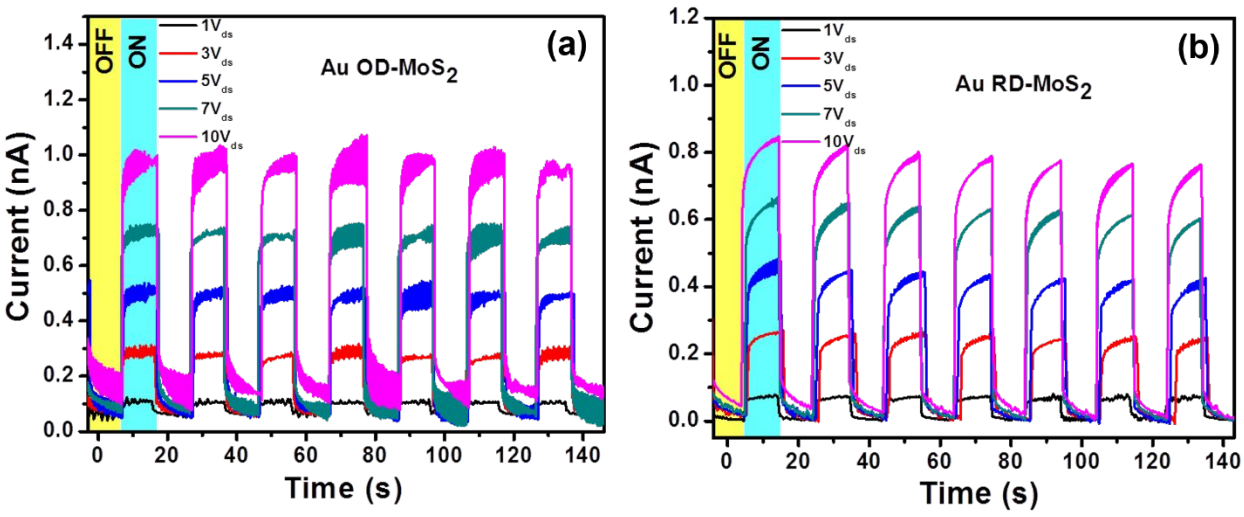

Figure S5: Time-dependent photocurrent measurements of bilayer MoS_2 that is decorated with a) Au OD; b) RD nanostructures and studied at various bias voltages (V_{ds} = 1, 3, 5, 7, and 10 V) with a constant laser power density of 318.471 mW/cm^2.

f) Photodetection of MoS_2 hybridized with Au nanorod:

The Plots of the photocurrent versus the illumination power (V_{ds} = 3 V) for MoS_2 that is hybridized with Au nanorods and nanocubes are shown in Figure S6a. In addition, the photoresponsivity measurements of hybrid MoS_2 bilayer that is decorated with Au nanorods and excited at 520 nm and 634 nm with various bias voltages (V_{ds} = 1,3,5,7,10 V) are shown in Figures S6 b & c, which again demonstrate the reproducibility of our device.

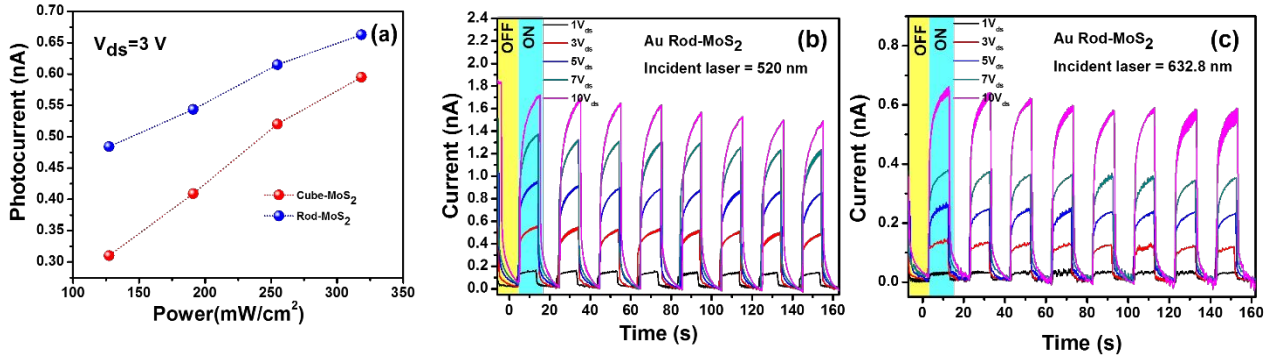

Figure S6: a) Plot of photocurrent versus laser power intensity at V_{ds} = 3 V for bilayer MoS_2 that is decorated with Au nanocubes and nanorods; b) and c) Time-dependent photocurrent measurements of bilayer MoS_2 that is decorated with Au nanorods and studied at various bias voltages (V_{ds} = 1, 3, 5, 7, and 10 V) with illumination by a 520 nm and 634 nm laser with a power density of 318.471 mW/cm^2.

g) Band structure modification and charge transfer of MoS_2 by hybridizing with Au.

Figure S7a shows the Fermi level shift of MoS_2 hybridized with Au toward the conduction band with a new isolated energy level that is formed in the bandgap, thereby reducing the interfacial Schottky barrier between Au and MoS_2[3]. In order to gain more insight into the exciton and plasmon coupling, time-resolved photoluminescence (TR-PL) measurements have been carried out for MoS_2 and MoS_2 decorated with Au nanoparticles as shown in Figure S7b. The PL decay time of as-grown MoS_2 is

4.483 ns, but it shortens to 3.183 ns when MoS_2 decorated with Au nanoparticles. This shorten decay time results from the charge transfer between Au and MoS_2[4].

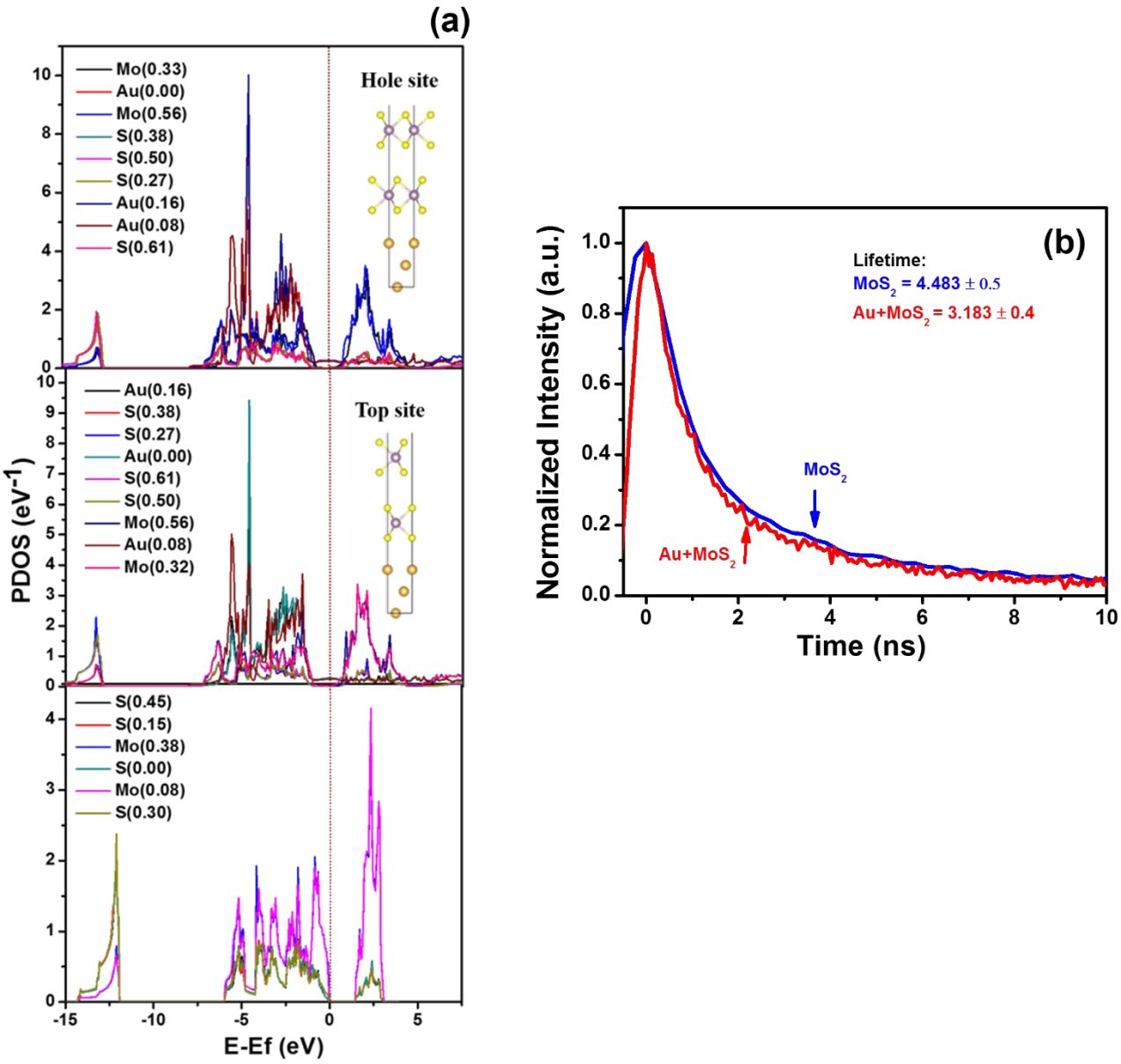

Figure S7: a) Partial density of states (PDOS) of MoS_2 and Au-MoS_2 hybrid by first-principle calculations; b) Time resolved photoluminescence spectra of MoS_2 and Au-MoS_2.

h) X-ray photoelectron spectroscopy (XPS) study for MoS_2 hybridized with Au.

In order to understand hybridization nature of bilayer MoS_2 with Au plasmonic nanostructures, we performed the X-ray photoelectron spectroscopy (XPS) as discussed in Figure S8. The binding energies of Mo 3d and S 2p are shifted by ca. 0.23 and 0.7 eV compared to pristine bilayer MoS_2. Whereas binding energies for Au 4f $_{7/2}$ and Au 4f $_{5/2}$ are 83.47 eV and 89.8 eV, respectively. This shows that there is no chemical interaction between pristine MoS_2 and Au/ MoS_2. The peak shift confirms the synergetic effect and charge transfer between MoS_2 and Au.

Plasmonic integrated MoS_2	Thickness/ No. of MoS_2 layers	FET	Wavelength (nm)	Photocurrent	Responsivity
Exfoliated MoS_2 with Au electrode[5]	7nm-10 nm	Yes	500-1550	~ 60 nA @ 532 nm	-
Exfoliated MoS_2- Au resonating and non-resonating nanostructures[6]	Bilayer	-	532, 1070	~ 5 pA @ 1080 nm	5.2 A W^{-1} @ 1070 nm 1.1× 10^5 A W^{-1} @ 532 nm
Exfoliated MoS_2- Au nanostructures[7]	4.5nm	Yes	477-720	4.6 µA @ 532 nm	-
Exfoliated MoS_2- Au nanospheres[8]	4-5 layers	Yes	400-800	3 µA @ 514 nm	-
CVD grown MoS_2- Au core-shell	Monolayer	Yes	600-800	2.5 fold increase in photocurrent	~ 0.9 nA µW^{-1} @ 630 nm

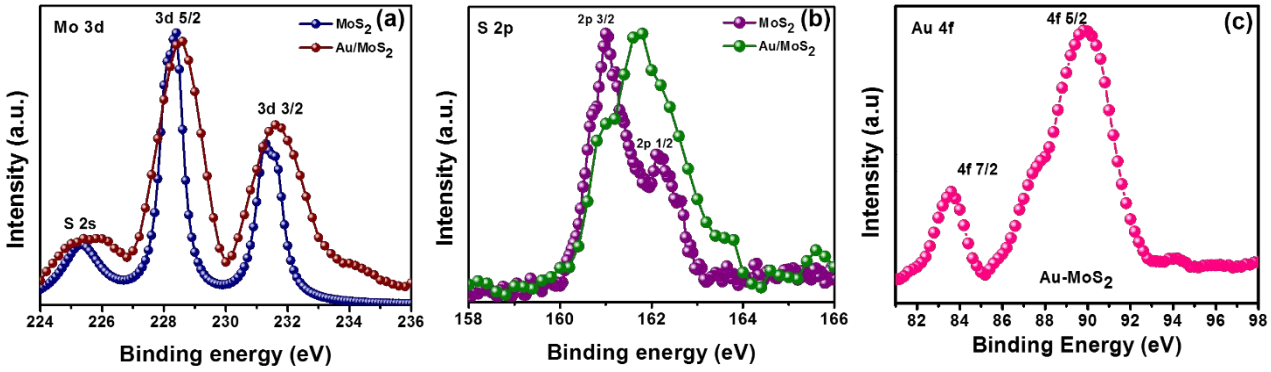

Figure S8: a) XPS spectra of MoS_2 and Au−MoS_2 in the (a) Mo 3d; (b) S 2p; and (c) Au 4f region

nanostructures[9]					
Exfoliated MoS_2-Pt nanostrips[10]	Bilayer	Yes	325, 532	~ 30 nA @ 325 nm	14 A W^{-1} @ 325 nm
CVD grown MoS_2-Ag nanowire network[11]	Monolayer	-	532	~ 0.8 µA @ 532 nm	0.15 A W^{-1} @ 532 nm
CVR grown MoS_2-Different Au nanostructures (Cube, OD,RD, Sphere, Rod)- ***Our work***	Bilayer	-	520 , 634	MoS_2 ~ 0.1 nA @ 520 nm MoS_2 / Au Cube ~ 1.4 nA @ 520 nm MoS_2 / Au OD ~ 1 nA @ 520 nm MoS_2 / Au RD ~ 0.8 nA @ 520 nm MoS_2 / Au Sphere ~ 0.4 nA @ 520 nm MoS_2 / Au Rod ~ 1.7 nA @ 520 nm @ 318.471 mW cm^{-2}	MoS_2 -cube Au NPs - 790 µA W^{-1} @ 532 nm; 0.159 mW cm^{-2}

Table.1 Performance metrics of plasmon enhanced MoS_2 photodetectors

References:

1. Tao J, Chai J, Lu X, Wong LM, Wong TI, Pan J*, et al.* Growth of wafer-scale MoS 2 monolayer by magnetron sputtering. *Nanoscale* 2015, **7**(6)**:** 2497-2503.

2. Kumar R, Sharma A, Kaur M, Husale S. Pt-Nanostrip-enabled plasmonically enhanced broad spectral photodetection in bilayer MoS2. *Adv Opt Mater* 2017, **5**(9).

3. Cheng W, Su H, Tang F, Che W, Huang Y, Zheng X*, et al.* Synergetic enhancement of plasmonic hot-electron injection in Au cluster-nanoparticle/C 3 N 4 for photocatalytic hydrogen evolution. *J Mater Chem* 2017, **5**(37)**:** 19649-19655.

4. Pan J, Chen J, Zhao D, Huang Q, Khan Q, Liu X*, et al.* Surface plasmon-enhanced quantum dot light-emitting diodes by incorporating gold nanoparticles. *Optics express* 2016, **24**(2)**:** A33-A43.

5. Hong T, Chamlagain B, Hu S, Weiss SM, Zhou Z, Xu Y-Q. Plasmonic hot electron induced photocurrent response at MoS2–metal junctions. *ACS nano* 2015, **9**(5)**:** 5357-5363.

6. Wang W, Klots A, Prasai D, Yang Y, Bolotin KI, Valentine J. Hot electron-based near-infrared photodetection using bilayer MoS2. *Nano letters* 2015, **15**(11)**:** 7440-7444.

7. Miao J, Hu W, Jing Y, Luo W, Liao L, Pan A*, et al.* Surface plasmon-enhanced photodetection in few layer MoS2 phototransistors with Au nanostructure arrays. *Small* 2015, **11**(20)**:** 2392-2398.

8. Lin J, Li H, Zhang H, Chen W. Plasmonic enhancement of photocurrent in MoS2 field-effect-transistor. *Applied Physics Letters* 2013, **102**(20)**:** 203109.

9. Sobhani A, Lauchner A, Najmaei S, Ayala-Orozco C, Wen F, Lou J*, et al.* Enhancing the photocurrent and photoluminescence of single crystal monolayer MoS2 with resonant plasmonic nanoshells. *Applied Physics Letters* 2014, **104**(3)**:** 031112.

10. Kumar R, Sharma A, Kaur M, Husale S. Pt-Nanostrip-Enabled Plasmonically Enhanced Broad Spectral Photodetection in Bilayer MoS2. *Advanced Optical Materials* 2017, **5**(9).

11. Bang S, Duong NT, Lee J, Cho YH, Oh HM, Kim H*, et al.* Augmented Quantum Yield of a 2D Monolayer Photodetector by Surface Plasmon Coupling. *Nano letters* 2018, **18**(4)**:** 2316-2323.